Applied Water Science (2019) 9:31
https://doi.org/10.1007/s13201-019-0907-y

ORIGINAL ARTICLE

Potentials of *Canarium schweinfurthii* seed shell as a novel precursor for CH_3COOK activated carbon: statistical optimization, equilibrium and kinetic studies

Zaharaddeen N. Garba[1] · M. Hazwan Hussin[2] · Ahmad Galadima[3] · Ibrahim Lawan[4]

Received: 30 June 2018 / Accepted: 11 February 2019 / Published online: 23 February 2019

Abstract
The possibility of utilizing *Canarium schweinfurthii* seed shell (CSSS) as a precursor to optimally produce activated carbon was harnessed by physico-chemical activation. Carbon (IV) oxide (CO_2) and potassium acetate (CH_3COOK) were employed as physical and chemical activating agents, respectively. Its ability as an effective adsorbent was tested on aqueous solution by removing 2,4,6-trichlorophenol (2,4,6-TCP). Central composite design was employed for the optimization giving rise to activation temperature of 670 °C, activation time of 100 min and impregnation ratio of 2.43. The optimal adsorbent (CSSS-AC) can be classified as mesoporous with surface area of 925.77 $m^2\ g^{-1}$ and maximum adsorption capacity of 247.23 mg g^{-1}. Higher amount of 2,4,6-TCP was removed at low pH with Freundlich and pseudo-second-order models found to be the most appropriate isotherm and kinetic model, respectively, in describing the adsorption process. The results reveal that *C. schweinfurthii* seed shell could be recommended as a promising novel precursor for producing activated carbons with high surface area and potentially desirable 2,4,6-TCP removal capacity, using CH_3COOK as an effective activating agent.

Keywords *Canarium schweinfurthii* seed shell (CSSS) · Central composite design (CCD) · Potassium acetate (CH_3COOK) · 2,4,6-Trichlorophenol (2,4,6-TCP) · Adsorption

Introduction

Chlorophenols are group of hazardous compounds present in industrial wastewater that are popularly known to be toxic to living organisms and also contaminate environment (Sarnalk and Kanekar 1995; Wang et al. 2018). They are also pertinacious and carcinogenic with intense odour (Armenante et al. 1999; Tan et al. 2009). Discharging chlorophenols into aquatic environment represent a noteworthy source of environmental pollution. Adsorption (Afidah and Garba 2016; Alizadeh et al. 2017; Garba and Afidah 2015, 2016; Hussin et al. 2016; Madannejad et al. 2018), catalytic wet oxidation (Chaliha and Bhattacharyya 2008), biodegradation (Steinle et al. 2000), ozonation and electrochemical degradation (Lim et al. 2013) and reverse osmosis (Gogoi et al. 2018) are just few of the several treatment methods engaged for the chlorophenols removal from wastewater with adsorption being the most active and efficient among them (Garba and Afidah 2016; Garba et al. 2015a). Popularity of adsorption method is related to its simplicity in design, ability to remove high amount of contaminants as well as swift adsorption kinetics with the most widely used adsorbent being activated carbon (Lee et al. 2015; Lladó et al. 2015). Being the most popular and active adsorbent reported (Garba et al. 2015c; Salman 2014), activated carbons have a very big advantage in terms of industrial applications due to its flexible surface characteristics (Garba et al. 2015b, c; Hazzaa and Hussein 2015). However, their high cost in the market becomes a hindrance in their applicability for the treatment of industrial sewages and runoffs (Chang et al. 2014; Sivarajasekar and Baskar 2014). This prompted an increasing interest in using cheap and readily available materials as precursors for

✉ Zaharaddeen N. Garba
dinigetso2000@gmail.com

1 Department of Chemistry, Ahmadu Bello University, P.M.B. 1044, Zaria, Nigeria

2 School of Chemical Sciences, Universiti Sains Malaysia, 11800 Penang, Malaysia

3 Department of Chemistry, Federal University, P.M.B. 1001, Gusau, Nigeria

4 Department of Agricultural and Environmental Engineering, Bayero University Kano, Kano, Nigeria

activated carbon production (Andrade et al. 2015; Mendes et al. 2015). Numerous waste materials such as vilayti tulsi (Pardeshi et al. 2013), natural walnut shell (Çelebi and Gök 2017), waste tea (Garba et al. 2015b; Özbaş et al. 2013), marble waste (Bouamra et al. 2018), egg shell (Mashangwa et al. 2017), saw palmetto spent (Papegowda and Syed 2017) and coconut spathe (Prashanthakumar et al. 2018) have been transformed effectively into adsorbents on a laboratory scale.

Canarium schweinfurthii is very popular plant in Africa with its seed shell very cheaply available in Nigeria. An attempt was made in this work to explore the potentials of *Canarium schweinfurthii* seed shell (CSSS) in the preparation of activated carbon after preliminary studies revealed CSSS to contain high carbon and low ash content which makes it a good precursor material for preparing activated carbon as adsorbent. To make the work better and more accurate, we seek the help of an adequate experimental design. Experimental design is a very useful tool that is widely reported in optimizing the preparation conditions of activated carbons (Garba et al. 2016) usually applied to simultaneously optimize the impact of variables in improving characteristics performance as well as minimizing error (Nouri et al. 2012). Currently to the best of our knowledge, no study has been reported on the optimization of activated carbon preparation conditions from CSSS using central composite design (CCD), a subset of response surface methodology (RSM) for the removal of 2,4,6-TCP.

Therefore, revealing the potentials of CSSS as a new precursor by optimizing the activated carbon preparation conditions for the removal of 2,4,6-TCP using CH_3COOK as an activating agent constitutes the novelty of this work. The effects of preparation variables (activation temperature, activation time as well as impregnation ratio) were studied concurrently to obtain a high 2,4,6-TCP adsorption capacity as well as the maximum activated carbon yield possible from aqueous solution using CCD.

Methodology

Materials

Sigma-Aldrich supplied both the chemical activating agent (CH_3COOK) and adsorbate (2,4,6-TCP) which were used without further purifying them. The chemical formula of the adsorbate (Fig. 1) is $C_6H_3Cl_3O$ with molecular weight of 197.45 g mol^{-1}. Reagents of analytical grade were employed in this work with all the solutions prepared using deionized water. CSSS samples were obtained from Jos, Plateau State, Nigeria. The shells were washed, sun-dried and later crushed with a mechanical crusher in the Institute of Agricultural Research (IAR), Ahmadu Bello University, Zaria.

Fig. 1 Chemical structure of 2,4,6-trichlorophenol (2,4,6-TCP)

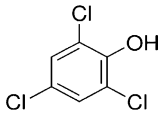

The crushed shells were sieved to a 250-µm particle size and dried in an oven at 100 °C for 24 h before usage.

Preparation of adsorbent (CSSS-AC)

The CSSS sample was dried, weighed then impregnated with CH_3COOK and later activated at temperature and time as determined by the design of experiment (DOE) in Table 1. The sample carbonization took place inside a furnace by transferring the mixture using a stainless steel vertical tubular reactor. Purified nitrogen gas (99.99%) atmosphere with the flow rate of 150 mL min^{-1} was used throughout in heating the reactor at 600 °C for the sample carbonization. The carbonization step was then followed by activation step which involved activating the carbonized sample under CO_2 gas at the same flow rate of 150 mL min^{-1} using similar reactor as used for carbonization under different temperatures and held for varying periods of time. The product was cooled to room temperature, then washed with distilled water until a neutral pH was attained, oven-dried and finally stored in an airtight container for further use.

The impregnation ratio was computed using the following relationship:

$$\text{Impregnation Ratio} = \frac{\text{weight of } CH_3COOK}{\text{weight of precursor (CSSS)}} \quad (1)$$

The adsorbent preparation was strictly adhered to the DOE table as shown in Table 1.

Design of experiments using response surface methodology

An orthodox RSM design, known as central composite design (CCD), was applied in this work to study the variables for preparing the activated carbons from CSSS in the same way as reported in our previously published works (Garba and Afidah 2014; Garba et al. 2014, 2015a).

The variables studied in this work were activation temperature coded as a_1, activation time coded as a_2 and impregnation ratio also coded as a_3 with their respective ranges chosen based on the literature as given in Table 2. The design-expert statistical software (version 8.0.6 Stat Ease, Inc., Minneapolis, MN 55413, USA) was employed for model fitting and significance for the CSSS-AC yield and adsorption capacity of the 2,4,6-TCP.

Table 1 Experimental design matrix for preparation of CSSS-AC and responses

Run	Level			CSSS-AC preparation variables				
				Temperature (°C)	Time (min)	IR	$Y_{2,4,6\text{-TCP}}$ (mg g^{-1})	$Y_{CSSS\text{-}AC}$ (%)
1	−1	−1	−1	611	73	0.77	48.9	26.05
2	+1	−1	−1	789	73	0.77	167.34	20.76
3	−1	+1	−1	611	197	0.77	54.2	24.9
4	+1	+1	−1	789	197	0.77	244.65	10.21
5	−1	−1	+1	611	73	2.43	236.17	20.05
6	+1	−1	+1	789	73	2.43	245.41	15.78
7	−1	+1	+1	611	197	2.43	212.72	21.92
8	+1	+1	+1	789	197	2.43	243.9	11.01
9	−1.682	0	0	550	135	1.60	42.44	25.69
10	+1.682	0	0	850	135	1.60	243.36	8.45
11	0	−1.682	0	700	30	1.60	170.04	25.83
12	0	+1.682	0	700	240	1.60	244.64	17.06
13	0	0	−1.682	700	135	0.20	31.08	28.11
14	0	0	+1.682	700	135	3.00	244.98	22.06
15	0	0	0	700	135	1.60	172.07	20.83
16	0	0	0	700	135	1.60	242.98	22.05
17	0	0	0	700	135	1.60	242.13	22.36
18	0	0	0	700	135	1.60	174.35	21.04
19	0	0	0	700	135	1.60	241.07	22.01
20	0	0	0	700	135	1.60	232.24	22.83

Table 2 Independent variables and their coded levels for the central composite design of *Canarium schweinfurthii* seed shells activated carbon (CSSS-AC) preparation

Adsorbent	Variables	Code	Unit	Coded variable levels				
				$-\alpha$	−1	0	+1	$+\alpha$
CSSS-AC	Activation temperature	a_1	°C	550	611	700	789	850
	Activation time	a_2	mins	30	73	135	197	240
	Impregnation ratio (IR)	a_3	–	0.20	0.77	1.60	1.60	3.00

Characterization of the prepared activated carbon

Scanning electron microscope (FEI QUANTA) was used to study the surface morphology of CSSS-AC with CHNS and thermogravimetric (Perkin Elmer TGA, USA) analyser employed in determining the elemental composition and proximate analysis, respectively. Brunauer–Emmett–Teller (BET) equation was employed to determine the BET surface area, micropore volume, total pore volume and pore size of the CSSS-AC.

Adsorption isotherms

Langmuir, Freundlich and Temkin isotherms are the three most popular isotherm models that were applied to fit the experimental data for the adsorption of 2,4,6-TCP. Langmuir isotherm equation describes an adsorption process that occurs upon a homogeneous surface where the adsorbate is distributed in monolayers (Kumar et al. 2010). It is mathematically described as:

$$\frac{C_e}{q_e} = \frac{1}{K_L Q_a^0} + \frac{C_e}{Q_a^0} \quad (2)$$

where C_e (mg L^{-1}) is the equilibrium concentration of the 2,4,6-TCP, q_e stands for the adsorbate amount adsorbed per unit adsorbent weight, while Q_a^0 (mg g^{-1}) and K_L (L mg^{-1}) are Langmuir constants related to maximum adsorption capacity and rate of adsorption, respectively. The essential characteristics of the Langmuir equation can be expressed in terms of dimensionless separation factor, R_L, defined as (Baccar et al. 2013):

$$R_L = \frac{1}{1 + K_L C_o} \quad (3)$$

where C_o is the highest initial solute concentration. R_L values indicate whether the adsorption is unfavourable

($R_L > 1$), linear ($R_L = 1$), favourable ($0 < R_L < 1$), or irreversible ($R_L = 0$).

Freundlich isotherm on the other hand assumes adsorption on heterogeneous surface with sites of different affinities (Hameed et al. 2008). The logarithmic form of the Freundlich isotherm is given by the following equation:

$$\log q_e = \log K_F + \frac{1}{n} \log C_e \tag{4}$$

where K_F and n are Freundlich constants. K_F ($mg^{1-n}\ g^{-1}\ L^n$) is the adsorption capacity when the adsorbate equilibrium concentration equal to 1.00 mg L^{-1} (Oo et al. 2009) with n related to adsorption intensity (Wan Ngah et al. 2011). In general, $n > 1$ suggests that adsorbate is favourably adsorbed on the adsorbent. The higher the n value, the stronger the adsorption intensity.

The influence of indirect adsorbent/adsorbate interactions on adsorption isotherms was illustrated by Temkin isotherm model (Hadi et al. 2010). It is written as:

$$q_e = \frac{RT}{b} \mathrm{In}A + \frac{RT}{b} \mathrm{In}C_e \tag{5}$$

where $\frac{RT}{b} = B$ (J/mol) and A (L/g) are Temkin constants, which are related to heat of sorption and maximum binding energy, respectively, R is the gas constant (8.31 J $mol^{-1}\ K^{-1}$), and T (K) is the absolute temperature.

Batch equilibrium and kinetic studies for the removal of 2,4,6-TCP

For the batch equilibrium and kinetic studies, 0.15 g of the CSSS-AC was placed in a set of 250 mL Erlenmeyer flasks with each flask containing 150 mL of 2,4,6-TCP solution. An isothermal shaker was used at 30 °C at a speed of 150 rpm until equilibrium was attained. The 2,4,6-TCP equilibrium concentration was determined using UV–Vis spectrophotometer (Helios γ) at maximum wavelength of 296 nm.

The percentage removal of 2,4,6-TCP (% R) was evaluated using the following equation.

$$\%R = \frac{C_o - C_e}{C_o} \times 100 \tag{6}$$

where C_o and C_e are the liquid-phase concentrations at initial and equilibrium states (mg L^{-1}), respectively.

The equilibrium amount of 2,4,6-TCP adsorbed per unit mass of adsorbent, q_e (mg g^{-1}), was estimated by equation as follows:

$$q_e = \frac{(C_o - C_e)V}{W} \tag{7}$$

where q_e (mg/g) is the equilibrium amount of adsorbate adsorbed per unit mass of adsorbent; V (L) is the volume of the solution; and W (g) is the mass of the adsorbent used.

In order to study the kinetics of the adsorption process, concentration of the 2,4,6-TCP solution was determined at intervals of time; the amount of the 2,4,6-TCP adsorbed at time t, q_t (mg g^{-1}), was calculated using equation:

$$q_t = \frac{(C_o - C_t)V}{W} \tag{8}$$

where C_o and C_t (mg L^{-1}) are the liquid-phase adsorbate concentrations at the initial and any time t, respectively.

The effect of initial pH (2–12) on the adsorption of the 2,4,6-TCP by the adsorbents was conducted by adjusting the pH of the solution with 0.1 M HCl and 0.1 M KOH solutions. The final pH of the solutions was measured using a pH meter (Martini instrument, Mi 106). The 2,4,6-TCP initial concentration was 350 mg L^{-1} with adsorbents dosage of 0.15 g at a temperature of 30 °C for 12 h. The % R was calculated using Eq. (6).

Results and discussion

Development of regression model equation

Table 1 presented the range of variables considered for CSSS-AC preparation with two responses ($Y_{2,4,6\text{-TCP}}$ and $Y_{CSSS\text{-AC}}$). Responses were correlated using CCD which led to the development of polynomial regression equations (all quadratic expressions). The model expression was selected in accordance with sequential model sum of square that is based on the polynomial's highest order where the model was not aliased and the additional terms were significant.

There was noticeable qualitative correlation between the predicted and experimental data as signified by the model's R^2 values of 0.9161 (2,4,6-TCP) and 0.9550 (yield) which were within suitability range (Sahu et al. 2010). The R^2 values for the adsorption capacity of 2,4,6-TCP and CSSS-AC yield were reasonably high and in good agreement with adjusted R^2 (Adj. R^2) values of 0.8405 and 0.9145, respectively, indicating reasonable agreement between the predicted values and the actual values. Equations 3 and 4 show the final empirical model's equations for the adsorption capacity of 2,4,6-TCP ($Y_{2,4,6\text{-TCP}}$) and CSSS-AC yield ($Y_{CSSS\text{-AC}}$) responses, respectively, given as

$$\begin{aligned} Y_{2,4,6-TCP} = {} & +216.76 + 50.32a_1 + 13.41a_2 + 57.32a_3 \\ & - 21.68a_1^2 + 1.11a_2^2 - 23.40a_3^2 + 11.74a_1a_2 \\ & - 33.56a_1a_3 - 13.45a_2a_3 \end{aligned} \tag{9}$$

$$Y_{CSSS-AC} = -88.63 + 0.37a_1 + 0.23a_2 - 13.58a_3 - 2.74a_1^2 - 1.63a_2^2 + 0.94a_3^2 - 3.60a_1a_2 + 8.08a_1a_3 + 0.02a_2a_3 \quad (10)$$

Antagonistic and synergetic effects of the respective variables are indicated by the negative and positive signs before the terms, respectively. Uni-factor, double factor and quadratic effects are indicated by the appearance of a single variable, two variables and second-order variables, respectively.

Statistical analysis

Tables 3 and 4 demonstrate the results of the surface quadratic model in the form of analysis of variance (ANOVA) for adsorption capacity of 2,4,6-TCP and CSSS-AC yield, respectively. To validate the significance and adequacy of the models, ANOVA is very essential. The sum of the squares of each of the variation sources, the model and the error variance were divided by the respective degrees of freedom to acquire the mean squares (Ahmad and Alrozi 2010b). The model terms are thought to be significant only if Prob. > F is less than 0.05. With respect to the adsorption capacity of 2,4,6-TCP from Table 3, the model was deemed to be significant due to F value of 12.13 and Prob. > F of 0.0003. In this case, the significant model terms were a_1, a_3, a_1^2, a_3^2 and a_1a_3; on the other hand, a_2, a_2^2, a_1a_2 and a_2a_3 were insignificant to the response ($Y_{2,4,6\text{-TCP}}$). The signal-to-noise ratio is gauged by adequate precision (AP). A ratio above 4 is appropriate. In this case, ratio of 10.92 for the adsorption capacity of 2,4,6-TCP signified an adequate signal which infers that his model can be used to steer the design space.

With respect to CSSS-AC yield from Table 4, the model F value and Prob. > F values were 23.58 and < 0.0001, respectively, signifying the model's significance. The significant model terms in this case were a_1, a_2, a_3, a_1^2 and a_1a_2 with a_2^2, a_3^2, a_1a_3 and a_2a_3 denoting the insignificant terms. Based on the adequate signal shown by AP (18.00), this model can be used to navigate the design space.

The ANOVA results obtained show the adequacy of both models [Eqs. (3) and (4)] in predicting the 2,4,6-TCP adsorption capacity as well as CSSS-AC yield, respectively, within the scope of variables studied. Additionally, Figs. 2 and 3 show the predicted values versus the experimental values for the 2,4,6-TCP adsorption capacity and CSSS-AC yield, respectively. The figures further proved the success of these developed models in effectively correlating the CSSS-AC preparation variables with the responses showing the closeness of the predicted values to the experimental values obtained.

Table 3 ANOVA for response surface quadratic model of 2,4,6-TCP adsorption capacity by CSSS-AC

Source	Sum of squares	Degree of freedom	Mean square	F value	Prob > F
Model	1.07×10^5	9	11,911.57	12.13	0.0003
a_1	34,580.85	1	34,580.85	35.20	0.0001
a_2	2455.17	1	2455.17	2.50	0.1450
$a3$	44,874.69	1	44,874.69	45.68	< 0.0001
a_1^2	6771.08	1	6771.08	6.89	0.0254
a_2^2	17.66	1	17.66	0.018	0.8960
a_3^2	7889.51	1	7889.51	8.03	0.0177
a_1a_2	1103.33	1	1103.33	1.12	0.3142
a_1a_3	9009.52	1	9009.52	9.17	0.0127
a_2a_3	1446.41	1	1446.41	1.47	0.2528
Residual	9823.51	10	982.35	–	–

A.P. 10.92; R^2 0.9196; Adj. R^2 0.8405

Table 4 The ANOVA for response surface quadratic model of CSSS-AC yield

Source	Sum of squares	Degree of freedom	Mean square	F value	Prob > F
Model	532.24	9	59.14	23.58	< 0.0001
a_1	301.37	1	301.37	120.17	< 0.0001
a_2	63.07	1	63.07	25.15	0.0005
a_3	39.87	1	39.87	15.90	0.0026
a_1^2	68.61	1	68.61	27.36	0.0004
a_2^2	5.81	1	5.81	2.32	0.1589
a_3^2	6.12	1	6.12	2.44	0.1492
a_1a_2	32.16	1	32.16	12.82	0.0050
a_1a_3	2.88	1	2.88	1.15	0.3091
a_2a_3	9.68	1	9.68	3.86	0.0778
Residual	25.08	10	2.51	–	–

A.P. 18.00; R^2 0.9550; Adj. R^2 0.9145

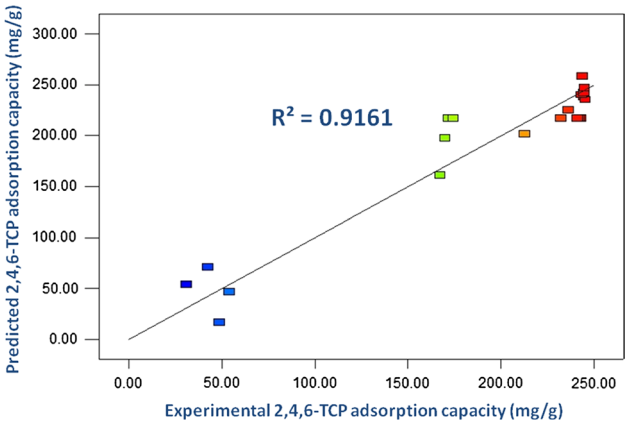

Fig. 2 Relationship between predicted and experimental data for 2,4,6-TCP adsorption capacity

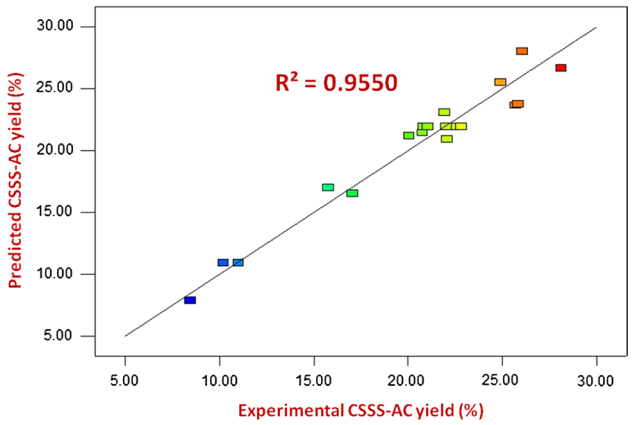

Fig. 3 Relationship between predicted and experimental data of CSSS-AC yield

Adsorption capacity of 2,4,6-TCP

From the ANOVA data generated in Table 3 with respect to the adsorption capacity 2,4,6-TCP, the three variables (activation temperature, time of activation and IR) can be seen to have uneven impact on the adsorption of 2,4,6-TCP onto the prepared CSSS-AC. The lowest effect was shown by the activation time (a_2) with F value of 2.50, and also its variation did not have a significant effect on the processes. The most significant effect inflicted on the adsorption capacity of 2,4,6-TCP came from individual factors of activation temperature (a_1) and IR (a_3) as well as their interactions (a_1a_3) as can be seen by their large F values of 35.20 and 45.68, respectively (Table 3). IR imposed the most significant effect on the adsorption capacity of 2,4,6-TCP by the CSSS-AC having the largest F value of 45.68 in comparison with other factors. The effect of activation temperature was the moderate and also significant showing F value of 35.20. As can be seen from Fig. 4 (A&B), there was a direct relationship between activation temperature and IR with the adsorption capacity of 2,4,6-TCP.

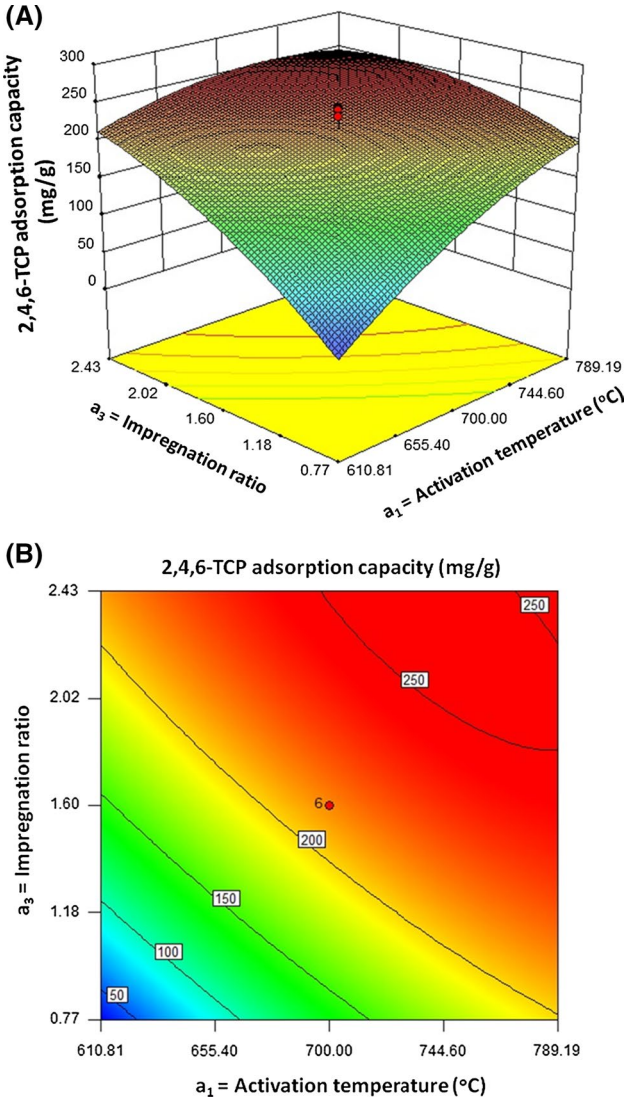

Fig. 4 Response surface plots of 2,4,6-TCP adsorption capacity by CSSS-AC; **a** 3D response surface plots demonstrating the effect of activation temperature and IR (activation time = 135 min) and **b** contour plots effect of the same variables on the 2,4,6-TCP adsorption capacity by CSSS-AC ($Y_{2,4,6\text{-TCP}}$)

CSSS-AC yield

The ANOVA data generated in Table 4 are with respect to the CSSS-AC yield. It can be observed that activation temperature (a_1) inflicted the greatest effect on CSSS-AC yield with the highest F value of 120.17, whereas activation time (a_2) and IR (a_3) show less impact on this response with F values of 25.15 and 15.90, respectively. The quadratic effect of activation temperature (a_1^2) was more pronounced with F value of 27.36, while that of activation time (a_2^2) and IR (a_3^2) were lower with F values of 2.32 and 2.44, respectively. The interaction effect between temperature and IR (a_1a_3) and that of interaction between activation time and IR (a_2a_3) were low with F values of 1.15 and 3.86, respectively, while that of interaction between activation temperature and activation time (a_1a_2) was more significant with F value of 12.82. Figure 5a shows the 3D response surface plots for the studied variables demonstrating the effect of temperature and time of activation with impregnation ratio fixed at zero level (IR = 1.60), whereas Fig. 4b shows the contour plots effect of the same variables on the CSSS-AC yield response (Y_{CSSS}). From both figures, the CSSS-AC yield was found to decrease with an increase in both temperature and time of activation.

Our preceding works on preparation of activated carbons from *Borassus aethiopum* shells (Garba et al. 2014), *Prosopis africana* seed hulls (Garba and Afidah 2014) and *Brachystegia eurycoma* seed hulls (Garba et al. 2015a) agreed very

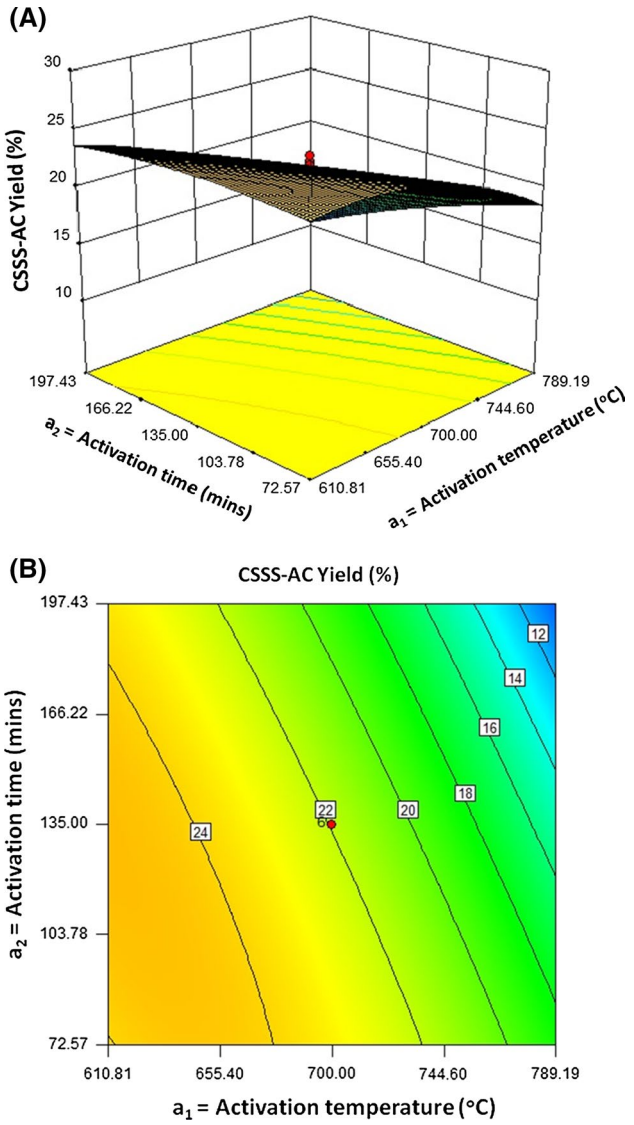

Fig. 5 Response surface plots of CSSS-AC yield; **a** 3D response surface plots demonstrating the effect of temperature and time of activation (IR = 1.60) and **b** contour plots effect of the same variables on the CSSS-AC yield response (Y_{CSSS})

well with the results obtained in this work. Other researchers like Sudaryanto et al. (2006), Hameed et al. (2009) and Tan et al. (2008) also reported similar observations, concluding less impact of activation time on the pore structure of activated carbon produced from cassava peel, oil palm fibre and coconut husk, respectively. They also reported noteworthy changes in the pore characteristics of their adsorbents due to the impact of activation temperature as well as the impregnation ratio. Sentorun-Shalaby et al. (2006) also reported activation time to show very negligible effect on the surface area of apricot stone activated carbon produced using steam as physical activating agent. However, according to Yang and Lua (2003), activation temperature and dwell time were the most significant parameters that affected the characteristics of pistachio-nut shell activated carbon.

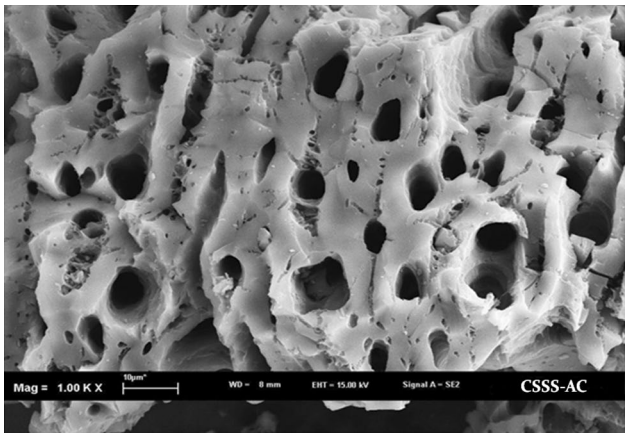

Fig. 6 Scanning electron micrograph (1000×) of the optimal activated carbon (CSSS-AC) prepared under optimum conditions (activation temperature of 670 °C, activation time of 100 min and IR of 2.43)

Process optimization

One of the main objectives of this study is to find the optimum process parameters in which CSSS-AC prepared should have large 2,4,6-TCP adsorption capacity as well as high carbon yield. Optimizing these responses under the same conditions is very complicated because the interest region of factors is poles apart since 2,4,6-TCP adsorption capacity is inversely proportional to the CSSS-AC yield; therefore, the function of desirability was applied using the design-expert software, in order to compromise between these responses. The target criteria were set as maximum values for the two responses. The predicted and experimental results of 2,4,6-TCP adsorption capacity and CSSS-AC yield obtained at optimum conditions are listed in Table 5.

Table 5 The CSSS-AC preparation parameters optimization

Model desirability	Activation temperature, a_1 (°C)	Activation time, a_2 (mins)	Impregnation ratio, a_3	2,4,6-TCP adsorption capacity (mg g^{-1})			CSSS-AC yield (%)		
				Predicted	Experimental	Error	Predicted	Experimental	Error
0.83	670	100	2.43	245.38	247.23	1.85	22.00	22.93	0.93

Table 6 Elemental contents and proximate analysis of the precursor (CSSS) sample and prepared activated carbon (CSSS-AC)

Sample	Elemental analysis (%)					Proximate analysis (%)			
	C	H	S	N	(Others)[a]	Fixed carbon	Volatile content	Moisture content	Ash content
Precursor (CSSS)	47.11	5.12	0.73	4.62	42.42	49.06	35.21	11.82	3.91
CSSS-AC	85.02	2.44	0.17	1.24	11.13	82.04	10.77	7.02	0.17

[a]Estimated by difference

Activation temperature of 670 °C, activation time of 100 min and IR of 2.43 were required to produce the optimal CSSS-AC giving rise to 2,4,6-TCP adsorption capacity of 247.23 mg g^{-1} and CSSS-AC yield of 22.93%. It is clear from Table 5 that the experimental values obtained were in good agreement with the values predicted from the models, with relatively small errors which were only 1.85 and 0.93 for 2,4,6-TCP adsorption capacity and CSSS-AC yield, respectively.

Characterization of the optimized CSSS-AC

Surface morphology

Figure 6 shows the SEM image of the CSSS-AC showing large and well-developed pores on its surface. This might be attributed to the effect of activation process used which comprised both CO_2 and CH_3COOK as physical and chemical activating agents, respectively. The high 2,4,6-TCP adsorption capacity could also be attributed to the well-developed pores on the CSSS-AC. Comparable observations were reported by other researchers utilizing *Borassus aethiopum* shells (Garba et al. 2014), *Prosopis africana* seed hulls (Garba and Afidah 2014), *Brachystegia eurycoma* seed hulls (Garba et al. 2015a), oil palm shell (Hamad et al. 2011) and

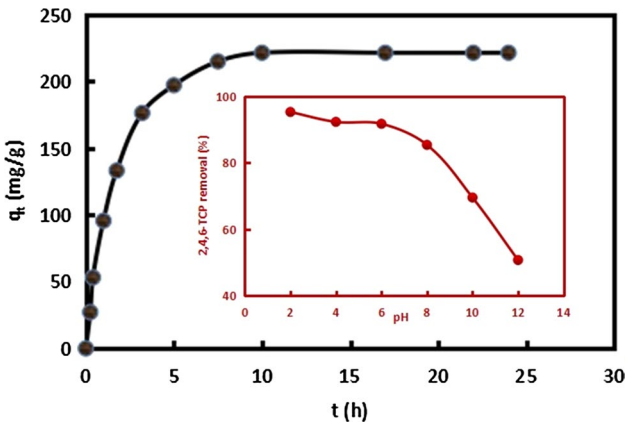

Fig. 7 Effect of contact time and pH (inset) on the removal of 2,4,6-TCP onto CSSS-AC

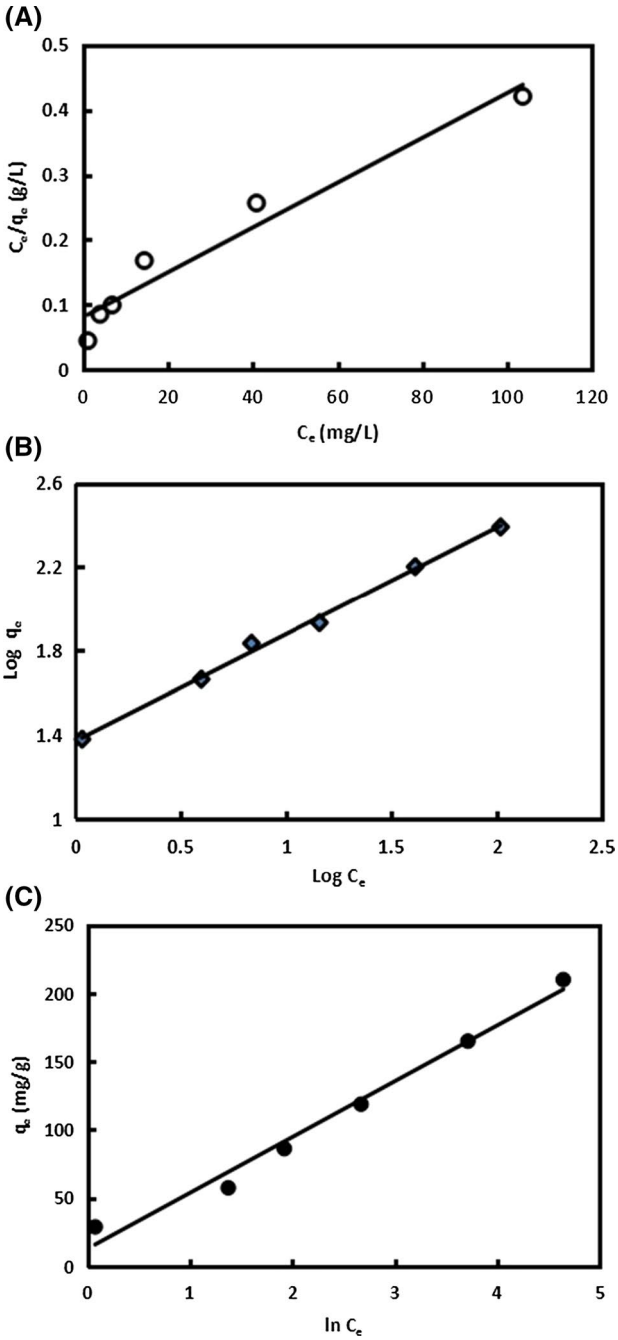

Fig. 8 **a** Langmuir isotherms, **b** Freundlich isotherms and **c** Temkin isotherms of the CSSS-AC for 2,4,6-TCP adsorption at 30 °C

mangosteen peel (Ahmad and Alrozi 2010a) as precursors for activated carbon.

Elemental/proximate analysis

The elemental/proximate analysis of CSSS and CSSS-AC is presented in Table 6. The precursor shows high carbon content divulging its potential to be utilized as a suitable precursor for activated carbon preparation. There was good agreement between carbon content of CSSS and some carbonaceous materials (Cordero et al. 2001) with the tremendous increase from 47.11 to 85.02% after its transformation into CSSS-AC. The sulphur content of the CSSS-AC was insignificant (0.17%) which is similar to mangosteen peel-based activated carbon reported by Ahmad and Alrozi (Ahmad and Alrozi 2010a). After the carbonization and activation process transformed CSSS into CSSS-AC, there was tremendous decrease in volatile matter content (35.21–10.77%), whereas the fixed carbon content increased from 49.06 to 82.04%. The increase in carbon content as well as the decrease in volatile matter content observed in Table 6 was attributed to pyrolytic effect at high temperature which leads to the degradation of organic substances, discharged both as gas and liquid tars leaving a material with high carbon purity (Ahmad and Alrozi 2010a). Another sign attributed to a good precursor material is low ash content which is sign of a tendency that the precursor can withstand high temperature treatment during carbonization cum chemical activation. CSSS has ash content 3.91% and hence can be classified as a good precursor.

CSSS-AC surface area and pore volume

The BET surface area, total pore volume, micropore volume and an average pore size of the CSSS-AC obtained were 925.77 $m^2\ g^{-1}$, 0.52 $cm^3\ g^{-1}$, 0.29 $cm^3\ g^{-1}$ and 3.62 nm, respectively, which lies in the mesopores region according to the IUPAC classification. Physico-chemical activation process which involved both CH_3COOK and CO_2 have big influence on the high BET surface area and total pore volume of the CSSS-AC. Carbonization process plays a key role in pore development as it leads to an increase in the BET surface area and pore volume of the activated carbon by promoting the diffusion of the activating agent molecules into the pores, thereby intensifying the CH_3COOK—carbon and CO_2—carbon reactions, which would then create more pores in the CSSS-AC (Stavropoulos and Zabaniotou 2005).

Effect of contact time and solution pH on the 2,4,6-TCP adsorption

Profiles portraying the impact of contact time and solution pH on the 2,4,6-TCP adsorption are presented in Fig. 7. The 2,4,6-TCP removal was rapid at the beginning, which then regressed slowly and steadily until an equilibrium time of about 7 h. This was attributed to availability of numerous vacant active sites on the adsorbent at the initial stage. The reduction in momentum of adsorption with time was due to saturation and reduction of the available active sites (Krishnan et al. 2011). The adsorption continued to be slow until a time when insignificant adsorption was observed, that is the dynamic equilibrium stage where the adsorption rate on the adsorbent surface was the same as the amount desorbed by the same surface. The above observations compared well with the literature. The adsorption of TCP on coconut shell-based commercial grade activated carbon needed 60–210 min for initial concentration of 10–100 mg L^{-1} (Radhika and Palanivelu 2006). About 10 h was also reported to be required for 200 mg L^{-1} concentrations of both 2,4-DCP and 2,4,6-TCP to reach equilibrium on their adsorption onto cattail fibre AC (Ren et al. 2011).

Table 7 Isotherm parameter constants for 2,4,6-TCP adsorption onto CSSS-AC at 30 °C

Parameter	Langmuir isotherm				Freundlich isotherm			Temkin isotherm		
	Q_a^0 (mg g^{-1})	K_L (L mg^{-1})	R_L	R^2	K_F ($mg^{1-n}\ g^{-1}\ L^n$)	n	R^2	A (L g^{-1})	B (J mol^{-1})	R^2
2,4,6-TCP	294.12	0.042	0.064	0.9527	23.415	1.961	0.9961	2.074	40.912	0.983

Table 8 Comparison of maximum monolayer adsorption capacity of 2,4,6-TCP adsorption on different adsorbents

Adsorbent	Adsorbate	Q_a^0 (mg g^{-1})	References
CSSS-AC	2,4,6-TCP	294.12	This work
Activated clay	2,4,6-TCP	123.46	Hameed (2007)
Commercial activated carbon	2,4,6-TCP	112.35	Radhika and Palanivelu (2006)
Coconut shell activated carbon	2,4,6-TCP	122.40	Radhika and Palanivelu (2006)
Chemically modified chitosan	2,4,6-TCP	80.26-375.94	Zhou et al. (2014)
Copper (II)–halloysite nanotubes	2,4,6-TCP	217.39	Zango et al. (2016)
Calcined kaolinite-biomass composites	2,4,6-TCP	4.4–14.1	Olu-Owolabi et al. (2017)

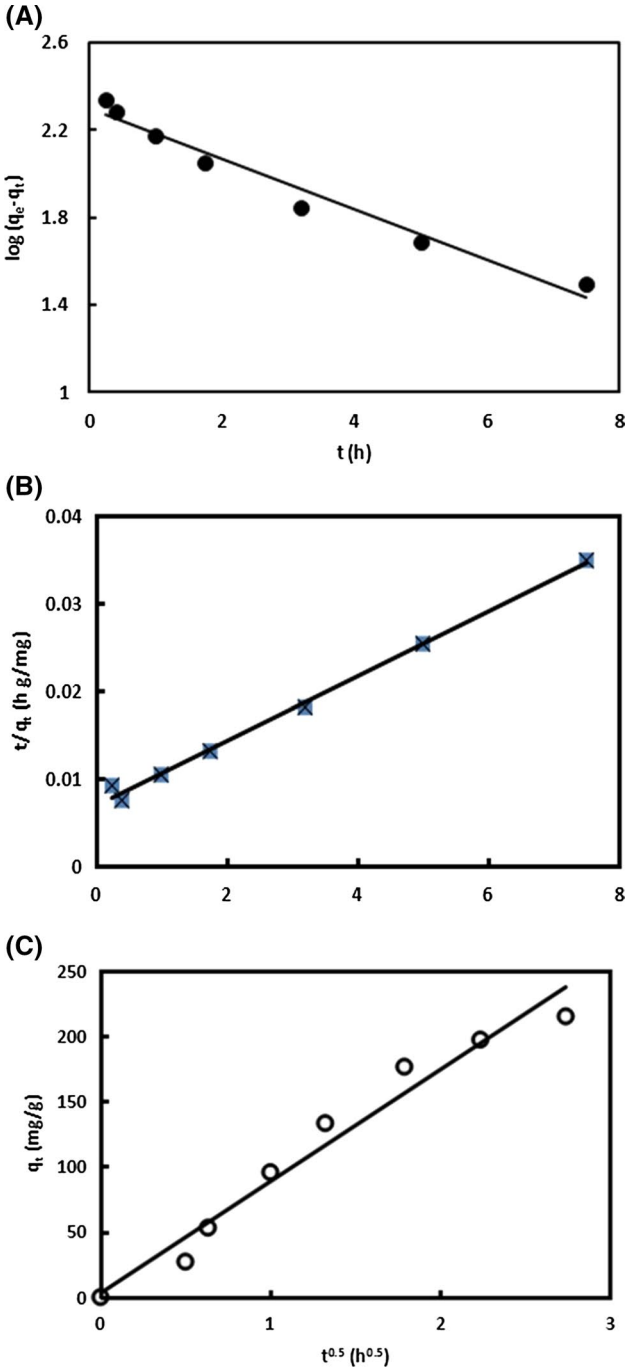

Fig. 9 **a** Pseudo-first-order, **b** pseudo-second-order and **c** intra-particle diffusion kinetic plots for 2,4,6-TCP adsorption onto CSSS-AC at 30 °C

The influence of solution pH on the adsorption of 2,4,6-TCP onto CSSS-AC is shown in Fig. 7 (inset). As can be observed from the plot, the percentage 2,4,6-TCP removal shows a significant decrease with an upsurge in the solution pH from 2 to 12. The highest removal on CSSS-AC was achieved at pH 2, with percentage removal as high as 95.34%. The significant decrease in 2,4,6-TCP percentage removal with an increase in the solution pH from 2 to 12 was attributed to the 2,4,6-TCP being a proton donor. According to (Hamad et al. 2010), at a certain pH (when the solution pH is greater than the pK_a of chlorophenols), they turn into anions, causing the negative charge of phenoxide ions to escalate thereby declining the adsorption due to a repulsive force between the phenoxide ions and negative groups on the surface (Hamad et al. 2010).

Equilibrium and kinetic data analysis

To analyse the equilibrium data, Langmuir, Freundlich and Temkin isotherm equations were plotted to determine the best fitted model. The respective plots are presented in Fig. 8a–c. The theoretical isotherm parameters Q_a^0, K_L, R_L, K_F, n, A, B and the correlation coefficients (R^2) obtained from those plots are listed in Table 7. From the Langmuir isotherm, the CSSS-AC can be seen to exhibit Q_a^0 value of 294.12 mg g^{-1}. This high value can be related to its porosity and surface area. Additionally from Table 7, CSSS-AC has R_L value of 0.064 which lies between 0 and 1, confirming that the adsorption is favourable under the studied conditions. The values of maximum monolayer adsorption capacity Q_a^0 obtained in this work compare well with some other adsorbents reported from literature as shown in Table 8.

Meanwhile, from the Freundlich isotherm model, CSSS-AC has n value of 1.961 which is greater than unity, confirming CSSS-AC as good adsorbent for 2,4,6-TCP removal. The data were also fitted for Temkin model, and the values of A and B were 2.074 L g^{-1} and 40.912 J mol^{-1}, respectively. Still from the fitting results listed in Table 7, Freundlich isotherm model with the highest R^2 value of 0.9961 appeared to be much more applicable than the Temkin (0.9830) and Langmuir (0.9527) isotherm models. This connotes that the 2,4,6-TCP molecules from bulk solution were not adsorbed on specific monolayer and is heterogeneous in nature.

In order to examine the characteristics and mechanism of the 2,4,6-TCP adsorption onto CSSS-AC, the adsorption kinetics data generated were fitted by the pseudo-first-order, pseudo-second-order and intra-particle diffusion kinetic models with their respective equations expressed as:

$$\log\left(q_e - q_t\right) = \log q_e - \frac{k_1}{2.303} \tag{11}$$

$$\frac{t}{q_t} = \frac{1}{k_2 q_e^2} + \frac{1}{q_e} t \tag{12}$$

$$q_t = k_{ip} t^{1/2} + C \tag{13}$$

Table 9 Kinetic models parameters for the adsorption of 2,4,6-TCP onto CSSS-AC at 30 °C

Parameter	Pseudo-first-order model				Pseudo-second-order model			Intra-particle diffusion model		
	$q_{e,exp}$ (mg g^{-1})	k_1 (h^{-1})	$q_{e,cal}$ (mg g^{-1})	R^2	k_2 (g mg^{-1} h)	$q_{e,cal}$ (mg g^{-1})	R^2	k_p (mg g^{-1} $h^{0.5}$)	C_2	R^2
2,4,6-TCP	246.33	0.266	199.480	0.9667	0.002	270.270	0.9948	85.560	2.879	0.9645

where q_e and q_t are the amounts of 2,4,6-TCP adsorbed (mg g^{-1}) at equilibrium and at time t (h), respectively, while k_1 (h^{-1}) and k_2 (g mg^{-1} h) are the adsorption rate constants of pseudo-first- and pseudo-second-order adsorption, respectively, k_{ip} is rate constant of the intra-particle diffusion equation, and C gives information about the boundary layer thickness: larger value of C is associated with the boundary layer diffusion effect. The fitting curves are shown in Fig. 9a–c with the kinetic parameters reported in Table 9. As can be observed from Table 9, the R^2 values for pseudo-first-order model (0.9667) and the intra-particle diffusion (0.9645) were not high. Additionally, the calculated q_e value with respect to pseudo-first-order model (199.480 mg g^{-1}) was not in good agreement with the experimental value (246.33 mg g^{-1}), indicating that pseudo-first-order is not the most appropriate kinetic model to rationalize the adsorption of 2,4,6-TCP onto CSSS-AC adsorbent. However, there was a better agreement between the experimental and calculated q_e values (270.270 mg g^{-1}) obtained from pseudo-second-order model with the R^2 value obtained also closer to unity (0.9948), confirming that the 2,4,6-TCP adsorption onto CSSS-AC adsorbent fitted better into the pseudo-second-order model.

Conclusions

Three preparation variables (activation temperature, activation time and IR) of CSSS-AC and their effects on two responses (2,4,6-TCP adsorption capacity and CSSS-AC yield) were studied by employing CCD, a subset of RSM. IR imposed the greatest effect on the adsorption capacity of 2,4,6-TCP with activation temperature showing the most significant effect on CSSS-AC yield. The optimum CSSS-AC preparation conditions obtained were activation temperature of 670 °C, activation time of 100 min and IR of 2.43 showing considerably high 2,4,6-TCP adsorption capacity as well as significantly good CSSS-AC yield. There was good agreement between the experimental values obtained with the values predicted from the models showing relatively small errors. The isotherm adsorption data fit well with Freundlich model and the kinetic data fit better with the pseudo-second-order model. The high maximum adsorption capacity of the adsorbent was attributed to CSSS-AC being mesoporous with considerably high BET surface area and well-developed pores on its surface, confirming potassium acetate (CH_3COOK) and *schweinfurthii* seed shell (CSSS) to be a promising activating agent and a low cost precursor, respectively, for activated carbon production.

Acknowledgements The authors are thankful to the Department of Chemistry, Ahmadu Bello University, Zaria, Nigeria, and School of Chemical Sciences, Universiti Sains Malaysia, for providing infrastructural facilities and active moral support towards completion of this work.

Author contributions ZNG, MHH, AG and IL designed the research; ZNG carried out the laboratory work and did the RSM modelling and statistical analyses; all the authors interpreted the results and participated in the writing of this research article.

Compliance with ethical standards

Conflict of interest The authors declare that they have no conflict of interest.

Availability of data and materials All data and materials relevant to this article have been included.

Consent for publication All authors have endorsed the publication of this research.

References

Afidah AR, Garba ZN (2016) Efficient adsorption of 4-chloroguiacol from aqueous solution using optimal activated carbon: equilibrium isotherms and kinetics modeling. J Assoc Arab Univ Basic Appl Sci 21:17–23

Ahmad MA, Alrozi R (2010a) Optimization of preparation conditions for mangosteen peel-based activated carbons for the removal of remazol brilliant blue r using response surface methodology. Chem Eng J 165:883–890

Ahmad MA, Alrozi R (2010b) Removal of malachite green dye from aqueous solution using rambutan peel-based activated carbon: equilibrium, kinetic and thermodynamic studies. Chem Eng J 171:510–516

Alizadeh N, Shariati S, Besharati N (2017) Adsorption of crystal violet and methylene blue on azolla and fig leaves modified with magnetite iron oxide nanoparticles. Intl J Environ Res 11:197–206

Andrade RC, de Almeida CF, Suegama PH, de Arrudaa EJ, Arroyo PA, de Carvalho CT (2015) Buriti palm stem as a potential renewable

source for activated carbon production. Environ Technol Innov 3:28–34

Armenante PM, Kafkewitz D, Lewandowski GA, Jou CJ (1999) Anaerobic–aerobic treatment of halogenated phenolic compounds. Water Resour 33:681–692

Baccar R, Blánquez P, Bouzid J, Feki M, Attiya H, Sarrà M (2013) Modeling of adsorption isotherms and kinetics of a tannery dye onto an activated carbon prepared from an agricultural by-product. Fuel Proces Technol 106:408–415

Bouamra F, Drouiche N, Abdi N, Grib H, Mameri N, Lounici H (2018) Removal of phosphate from wastewater by adsorption on marble waste: effect of process parameters and kinetic modeling. Intl J Environ Res 12:13–27

Çelebi H, Gök O (2017) Evaluation of lead adsorption kinetics and isotherms from aqueous solution using natural walnut shell. Intl J Environ Res 11:83–90

Chaliha S, Bhattacharyya KG (2008) Catalytic wet oxidation of 2-chlorophenol, 2,4-dichlorophenol and 2,4,6-trichlorophenol in water with Mn (II)-MCM41. Chem Eng J 139:575–588

Chang KL, Chen CC, Lin JH, Hsien JF, Wang Y, Zhao F, Chen ST (2014) Rice straw-derived activated carbons for the removal of carbofuran from an aqueous solution. New Carbon Mater 29(1):47–54

Cordero T, Marquez F, Rodriguez-Mirasol J, Rodriguez JJ (2001) Predicting heating values of lignocellulosics and carbonaceous materials from proximate analysis. Fuel 80:1567–1571

Garba ZN, Afidah AR (2014) Process optimization of $k_2c_2o_4$-activated carbon from prosopis africana seed hulls using response surface methodology. J Anal Appl Pyrolysis 107:306–312

Garba ZN, Afidah AR (2015) Adsorption of 4-chlorophenol onto optimum activated carbon from an agricultural waste. Int J Sci Resour 4(5):1931–1936

Garba ZN, Afidah AR (2016) Evaluation of optimal activated carbon from an agricultural waste for the removal of para-chlorophenol and 2,4-dichlorophenol. Proc Saf Environ Prot 102:54–63

Garba ZN, Afidah AR, Hamza SA (2014) Potential of borassus aethiopum shells as precursor for activated carbon preparation by physico-chemical activation; optimization, equilibrium and kinetic studies. J Environ Chem Eng 2:1423–1433

Garba ZN, Afidah AR, Bello BZ (2015a) Optimization of preparation conditions for activated carbon from brachystegia eurycoma seed hulls: a new precursor using central composite design. J Environ Chem Eng 3:2892–2899

Garba ZN, Shikin FBS, Afidah AR (2015b) Valuation of activated carbon from waste tea for the removal of a basic dye from aqueous solution. J Chem Eng Chem Res 2:623–633

Garba ZN, Zango ZU, Babando AA, Galadima A (2015c) Competitive adsorption of dyes onto granular activated carbon. J Chem Pharm Res 7:710–717

Garba ZN, Ugbaga NI, Amina KA (2016) Evaluation of optimum adsorption conditions for Ni (II) and Cd (II) removal from aqueous solution by modified plantain peels (MPP). Beni-Suef Univ J Basic Appl Sci 5:170–179

Gogoi S, Chakraborty S, Saikia MD (2018) Surface modified pineapple crown leaf for adsorption of Cr(VI) and Cr(III) ions from aqueous solution. J Environ Chem Eng 6:2492–2501

Hadi M, Samarghandi MR, McKay G (2010) Equilibrium two-parameter isotherms of acid dyes sorption by activated carbons: study of residual errors. Chem Eng J 160:408–416

Hamad BK, Noor AM, Afidah AR, Mohd Asri MN (2010) High removal of 4-chloroguaiacol by high surface area of oil palm shell-activated carbon activated with NaOH from aqueous solution. Desalination 257(1–3):1–7

Hamad BK, Ahmad MN, Afidah AR (2011) Removal of 4-chloro-2-methoxy phenol by adsorption from aqueous solution using oil palm shell carbon activated by k_2co_3. J Phys Sci 22:41–58

Hameed BH (2007) Equilibrium and kinetics studies of 2,4,6-trichlorophenol adsorption onto activated clay. Colloids Surf A Physicochem Eng Asp 307:45–52

Hameed BH, Tan IAW, Ahmad AL (2008) Adsorption isotherm, kinetic modeling and mechanism of 2,4,6-trichlorophenol on coconut husk-based activated carbon. Chem Eng J 144(2):235–244

Hameed BH, Tan IA, Ahmad AL (2009) Preparation of oil palm empty fruit bunch-based activated carbon for removal of 2,4,6-trichlorophenol: optimization using response surface methodology. J Hazard Mater 164(2–3):1316–1324

Hazzaa R, Hussein M (2015) Adsorption of cationic dye from aqueous solution onto activated carbon prepared from olive stones. Environ Technol Innov 4:36–51

Hussin MH, Pohan NA, Garba ZN, Kassim MJ, Afidah AR, Brosse N, Haafiz MKM (2016) Physicochemical of microcrystalline cellulose from oil palm fronds as potential methylene blue adsorbents. Int J Biol Macromol 92:11–19

Krishnan KA, Sreejalekshmi KG, Baiju RS (2011) Nickel(II) adsorption onto biomass based activated carbon obtained from sugarcane bagasse pith. Bioresour Technol 102:10239–10247

Kumar KV, Calahorro CV, Juarez JM, Sabio MM, Albero JS, Reinoso FR (2010) Hybrid isotherms for adsorption and capillary condensation of N_2 at 77 k on porous and non-porous materials. Chem Eng J 162:424–429

Lee LY, Chin DZB, Lee XJ, Chemmangattuvalappil N, Gan S (2015) Evaluation of abelmoschus esculentus (lady's finger) seed as a novel biosorbent for the removal of acid blue 113 dye from aqueous solutions. Proces Saf Environ Prot 94:329–338

Lim JW, Lim PE, Seng CE, Adnan R (2013) Simultaneous 4-chlorophenol and nitrogen removal in moving bed sequencing batch reactors packed with polyurethane foam cubes of various sizes. Bioresour Technol 129:485–494

Lladó J, Lao-Luque C, Ruiz B, Fuente E, Solé-Sardans M, Dorado AD (2015) Role of activated carbon properties in atrazine and paracetamol adsorption equilibrium and kinetics. Process Saf Environ Prot 95:51–59

Madannejad S, Rashidi A, Sadeghhassani S, Shemirani F, Ghasemy E (2018) Removal of 4-chlorophenol from water using different carbon nanostructures: a comparison study. J Mol Liq 249:877–885

Mashangwa TD, Tekere M, Sibanda T (2017) Determination of the efficacy of eggshell as a low-cost adsorbent for the treatment of metal laden effluents. Int J Environ Res 11:175–188

Mendes FMT, Aline CCM, Deiseane LM, Marlucy SO, Rondinele OM, Viridiana SF (2015) High surface area activated carbon from sugar cane straw. Waste Biomass Valor 6:433–440

Nouri S, Abad MD, Bahram M (2012) Adsorption studies of b-naphthol by untreated and treated activated carbon [optimizing of adsorption by central composite design (ccd)]. J Iran Chem Soc 9:397–405

Olu-Owolabi BI, Alabi AH, Diagboya PN, Unuabonah EI, Düring R-A (2017) Adsorptive removal of 2,4,6-trichlorophenol in aqueous solution using calcined kaolinite-biomass composites. J Environ Manag 192:94–99

Oo CW, Kassim MJ, Pizzi A (2009) Characterization and performance of rhizophora apiculata mangrove polyflavonoid tannins in the adsorption of copper (II) and lead (II). Ind Crops Prod 30:152–161

Özbaş EE, Öngen A, Gökçe EC (2013) Removal of astrazon red 6b from aqueous solution using waste tea and spent tea bag. Desalin Water Treat 51:7523–7535

Papegowda PK, Syed AA (2017) Isotherm, kinetic and thermodynamic studies on the removal of methylene blue dye from aqueous solution using saw palmetto spent. Int J Environ Res 11:91–98

Pardeshi SD, Sonar JP, Zine AM, Thore SN (2013) Kinetic and thermodynamic study of adsorption of methylene blue and rhodamine b on adsorbent prepared from *Hyptis suaveolens* (vilayti tulsi). J Iran Chem Soc 10:1159–1166

Prashanthakumar TKM, Kumar SKA, Sahoo SK (2018) A quick removal of toxic phenolic compounds using porous carbon prepared from renewable biomass coconut spathe and exploration of new source for porous carbon materials. J Environ Chem Eng 6:1434–1442

Radhika M, Palanivelu K (2006) Adsorptive removal of chlorophenols from aqueous solution by low cost adsorbent–kinetics and isotherm analysis. J Hazard Mater 138(1):116–124

Ren L, Zhang J, Li Y, Zhang C (2011) Preparation and evaluation of cattail fiber-based activated carbon for 2,4-dichlorophenol and 2,4,6-trichlorophenol removal. Chem Eng J 168(2):553–561

Sahu JN, Acharya J, Meikap BC (2010) Optimization of production conditions for activated carbons from tamarind wood by zinc chloride using response surface methodology. Bioresour Technol 101(6):1974–1982

Salman JM (2014) Optimization of preparation conditions for activated carbon from palm oil fronds using response surface methodology on removal of pesticides from aqueous solution. Arab J Chem 7:101–108

Sarnalk S, Kanekar P (1995) Bioremediation of colour of methyl violet and phenol from a dye-industry waste effluent using *pseudomonas* spp. Isolated from factory soil. J Appl Bacteriol 79:459–469

Şentorun-Shalaby ÇD, Uçak-Astarlıog˘Lu MG, Artok L, Sarıcı Ç (2006) Preparation and characterization of activated carbons by one-step steam pyrolysis/activation from apricot stones. Microporous Mesoporous Mater 88:126–134

Sivarajasekar N, Baskar R (2014) Adsorption of basic red 9 on activated waste *Gossypium hirsutum* seeds: process modeling, analysis and optimization using statistical design. J Ind Eng Chem 20:2699–2709

Stavropoulos GG, Zabaniotou AA (2005) Production and characterization of activated carbons from olive-seed waste residue. Microporous Mesoporous Mater 82:79–85

Steinle P, Thalmann P, Hohener P, Hanselmann KW, Stucki G (2000) Effect of environmental factors on the degradation of 2,6 dichlorophenol in soil. Environ Sci Technol 34:771–775

Sudaryanto Y, Hartono SB, Irawaty W, Hindarso H, Ismadji S (2006) High surface area activated carbon prepared from cassava peel by chemical activation. Bioresour Technol 97:734–739

Tan IAW, Ahmad AL, Hameed BH (2008) Preparation of activated carbon from coconut husk: optimization study on removal of 2,4,6-trichlorophenol using response surface methodology. J Hazard Mater 153(1–2):709–717

Tan IAW, Ahmad AL, Hameed BH (2009) Adsorption isotherms, kinetics, thermodynamics and desorption studies of 2,4,6-trichlorophenol on oil palm empty fruit bunch-based activated carbon. J Hazar Mater 164(2–3):473–482

Wan Ngah WS, Fatinathan S, Yosop NA (2011) Isotherm and kinetic studies on the adsorption of humic acid onto chitosan-H_2SO_4 beads. Desalination 272:293–300

Wang B, Gao B, Wan Y (2018) Entrapment of ball-milled biochar in ca-alginate beads for the removal of aqueous Cd(II). J Ind Eng Chem 61:161–168

Yang T, Lua AC (2003) Characteristics of activated carbons prepared from pistachio-nut shells by potassium hydroxide activation. Microporous Mesoporous Mater 63:113–124

Zango ZU, Garba ZN, Abu Bakar NHH, Tan WL, Abu Bakar M (2016) Adsorption studies of Cu^{2+}–hal nanocomposites for the removal of 2,4,6-trichlorophenol. Appl Clay Sci 132–133:68–78

Zhou L-C, Meng X-G, Fu J-W, Yang Y-C, Yang P, Mia C (2014) Highly efficient adsorption of chlorophenols onto chemically modified chitosan. Appl Surf Sci 292:735–741